The Twenty-Second International Symposium on Artificial Life and Robotics 2017 (AROB 22nd 2017),
The Second International Symposium on BioComplexity 2017 (ISBC 2nd 2017),
B-Con Plaza, Beppu, Japan, January 19-21, 2017

Prediction of needle deflection based on reaction force analysis for needle puncture robot with CT equipment

Takayuki Matsuno[1], Kohei Sugiyama[1], Akisato Nagao[1], Tetsushi Kamegawa[1], Takao Hiraki[2], and Mamoru Minami[1]

[1]Okayama University, Japan
[2]Okayama University Hospital, Japan
(Tel: 81-86-251-8234)
[1]matsuno@cc.okayama-u.ac.jp

Abstract: There is a surgical method called Interventional Radiology (IR). This surgical method is conducted with imaging modality such as CT and X-rays. As compared with conventional survey, IR can be conducted in local anesthesia and this surgical method is minimally-invasive to patients. Recently IR is conducted by surgeons using a forceps and a needle. The minimum size of malignancy is approximately 3mm in diameter. Therefore operator must puncture a needle into body of patients accurately. Because operators conduct procedure close to the CT gantry, operators are exposure to radiation during CT scanning. In order to prevent radiation exposure, operators wear radiation protection aprons and handle a needle using a forceps. However, it is impossible to prevent radiation exposure completely. Zerobot which we have been developing aims to conduct whole process from positioning robot to inserting a needle by remote controlled operation. In this research, Zerobot for clinical assessment has been developed already, and animal experiment using animal has been performed. An effect on performance of Zerobot caused by deflection of skin and moving body tissue should be confirmed. Therefore experiment with animal is conducted. In this paper, overview of robotic IR and animal puncture experiment are described. Zerobot has sometimes succeeded to insert a needle into animal body tissue. When a needle is inserted to animal, the needle sometimes deflects because animal body tissue is soft. And trajectory of needle is affected by this problem. We can conjecture that this problem occurs also at the time of inserting needle to human. When a needle penetrate surface skin, destruction of spring property of skin was confirmed. In order to detect deflection of needle, magnitude of lateral force is significant. If inclination of lateral force increases along insertion depth, it is expected that the system can predict deflection during inserting needle.

Keywords: Interventional radiology, Needle insertion, teleoperated robot

1 INTRODUCTION

There is a surgical method called Interventional Radiology (IVR) [1]. This surgical method is conducted with imaging modality such as CT and X-rays. With observing medical images, the surgeon conducts IVR treatment percutaneously with inserting a needle or a catheter to the patient body. In particular, CT equipment has high visibility and objectivity. And CT fluoroscopy system ,which can show medical images in real time, is superior as guiding tool for IVR. So CT-guided IVR is applied to lung cancer treatment, liver cancer treatment, biopsy, and so on [2]. The situation of actual procedure is shown in Fig. 1. As compared with conventional survey, IVR can be conducted in local anesthesia and this surgical method is minimally-invasive to patients. Moreover patients can be discharged from the hospital about 3 or 4days after treatment. Because of these advantages, IVR is paid much attention in recent years.

Rencetly IVR is conducted by surgeons using a forceps and a needle. The size of malignancy is about 3mm in diameter[3]. Therefore operator must puncture a needle carefully and accurately. Because operators conduct procedure close to the CT gantry, operators are exposure to radiation during CT scanning. In order to prevent radiation exposure, operators wear radiation protection aprons and handle a needle using a forceps. However, it is impossible to prevent radiation exposure completely. Then some medical robots are developed in order to improve accuracy of positioning of a needle, and to reduce radiation exposure, such as Acubot[4], CTbot[5], and B-Rob[6]. These robots aim to support operators to insert a needle as CT-guided puncture. However, IVR

Fig. 1. Interventional Radiology

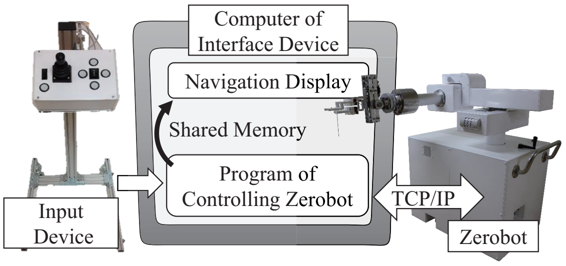

Fig. 2. System Structure of Robotic IVR

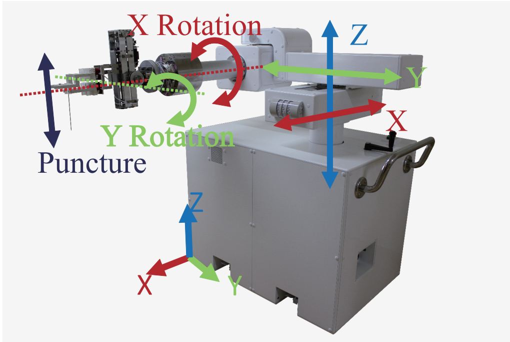

Fig. 3. IVR Robot

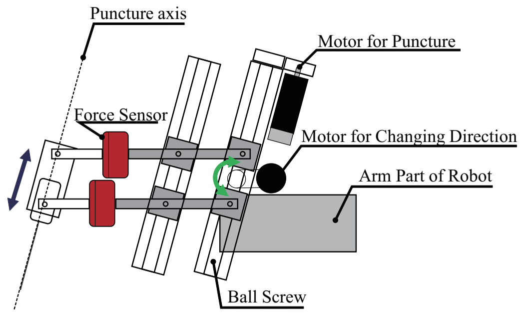

Fig. 4. End-effector of IVR Robot

robot, which is developed by us, aims to conduct whole process (from positioning robot to inserting a needle) by remote-control. In this research, prototype robot has been developed already, and animal experiment using rabbit has been performed.

This paper presents overview of Robotic IVR and result of animal experiment. In section II, overview which includes the mechanism of robot, procedure of puncture, interface and system structure is described. The result of animal experiment used IVR robot which is developed is described in section III. Finally, conclusion is provided in section IV.

2 OVERVIEW OF ROBOTIC IVR

2.1 System Structure

This subsection shows the system structure of Robotic IVR. Overview of the structure is shown in Fig.2. The robot is connected to PC with input device by LAN cable to communicate through TCP/IP. As receive the information of status of controller, PC with input device instructs to robot to actuate axes. The robot sends the values of all actuators and force sensor to PC. In the PC, program of controlling robot and navigation display is divided, and status of robot received by program of controlling robot is sent by TCP/IP communication to program of navigation display.

2.2 Mechanism

The appearance of CT-IVR robot is shown in Fig. 3. It has five DoF for needle tip position and needle orientation, and has one DoF in puncturing direction. There are six actuators in the robot. Four linear actuators (X,Y,Z and puncturing axis directions) and two rotational actuators (around the X and Y axis) are included. Therefore, IVR robot can perform puncture operation by actuating the puncturing axis for all of robot posture. Four wheels are mounted on the bottom of the robot, so it can be moved with human power. At the surgical operation, robot is located under a bed and fixed by locking the wheels. Changing needle orientation and puncturing are performed in CT-gantry by arm part above patient.

Because of structure of CT equipments, if metal part was in the gantry plane, incorrect image called artifact appears on CT image. If artifact appeared, a patient's internal image is obscured and trouble occurs on an surgical operation. Therefore, metal parts cannot be used on needle gripper. Accordingly parts are made of engineering plastic. In addition, puncturing motor and changing orientation motor is detached from CT radiography plane by adopting parallel link mechanism at end-effector, as shown in Fig. 4. Front of a part of gripping needle made of engineering plastic, two force sensors is located. These sensors can measure the moment around three axes. Using these devices, reaction force from skin is calculated and analyzed.

2.3 Procedure of Puncture

This subsection shows procedure of puncture using IVR robot. The procedure is listed bellow.

1. CT radiography
   Target tumor's position is confirmed from patient's CT image.
2. Planning
   Relation between metal marker on skin and tumor position is confirmed by CT image, and plan of puncture is decided. Then, puncturing point on surface of skin is pointed by marker pen.
3. Adjustment of Needle Tip Position and Needle Orientation

The Twenty-Second International Symposium on Artificial Life and Robotics 2017 (AROB 22nd 2017),
The Second International Symposium on BioComplexity 2017 (ISBC 2nd 2017),
B-Con Plaza, Beppu, Japan, January 19-21, 2017

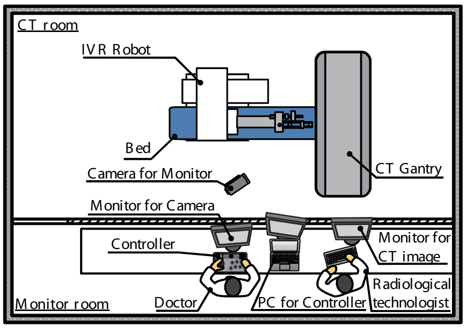

Fig. 5. Environment of Animal Experiment

Needle is brought to CT radiography plane based on lighting guide emitted from CT equipment. And needle tip position is adjusted to marked position on surface of skin. Moreover, needle orientation is adjusted to decided angle.

4. Fine Adjustment
   Needle orientation is made fine adjustments so as to direct the needle toward the target tumor, under CT guidance. Artifact from needle can be regarded as extension line of needle.
5. Puncture
   The needle is punctured. When the depth of puncture reaches the preplanned length, relation between needle tip and target tumor position is confirmed by CT radiography. And then, either needle tip position or needle orientation is operated as necessary.

The robot is operated in this procedure. If robot cannot manipulate needle accurately, the surgeon have to readjust the posture of needle based on real time CT image. It increases patient's radiation exposure. Therefore, accuracy of robot hand position is important.

2.4 Input device

Developed input interface is shown in Fig. 2 left side. This interface consists of nine push buttons and a joystick. Right half of input panel, which is further on the right side than joystick, corresponds to actuate linear axis of X, Y and Z of IVR robot. On the other hand, Left half of input panel which includes joystick corresponds to rotate around axis of X and Y, and to actuate axis of puncture. And speed of actuator is switchable so that needle puncture speed can be increased at the moment of penetrating surface of skin.

3 ANIMAL EXPERIMENT

In order to confirm the problem on conducting Robotic IVR, puncture experiment is important. CT-IVR phantom[7] puncture experiment is conducted as dry run of Robotic IVR. However reproducing an effect on needle caused by deflection or softness of human skin is difficult. An effect on performance of robot caused by deflection of skin and moving body tissue should be confirmed. Therefore animal experiments with rabbit were conducted.

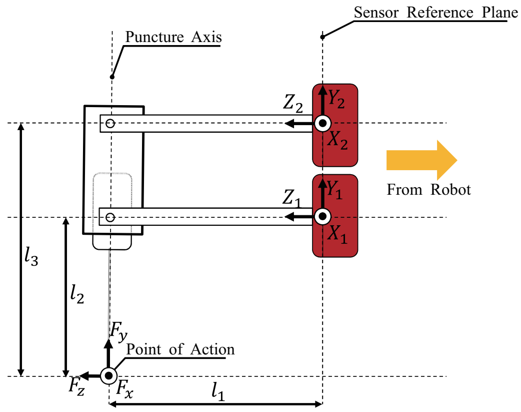

Fig. 6. Layout Drawing of Force Sensor

3.1 Environment of Animal Experiment

This subsection shows the environment of animal experiment. The experiments were conducted at Okayama Medical Innovation Center, Okayama University. Environment of the experiment is shown in Fig. 5. The rabbit is fixed on the bed, shaved body hair and scanned CT image. The doctor designated some rabbit's body tissues from CT image, and marked needle inserting point on the rabbit's skin. And then, puncture to the rabbit is performed following the procedure of subsection 2.3. Length of the needle which was used in this experiment is 75[mm], and diameter of the needle is 20 gauge (approx. 0.81[mm] diam.). Diameter of needle which includes needle guide is approx 1.1[mm]. And the needle is made of stainless steel.

Mount of force sensors is shown in Fig. 6. Each sensor can measure the moment around axis of X_i, Y_i and Z_i $(i = 1, 2)$. Using the moment values measured by two sensors, puncture reaction force is calculated. When F_x, F_y and F_z are applied to the point of action, F_x effects to values of M_{yi} and M_{zi}. On the other hands, F_y and F_z effects to values of M_{xi}. So we can calculate the value of F_x from M_{yi} and M_{zi}. But F_y and F_z should be calculated from only value of M_{xi}, so we cannot determine these values uniquely. In order to calculate these values uniquely, we assume that the value of F_z is almost zero because we confirmed the needle was always on CT image plane during puncture. Then equations (1) to (3) can be derivated.

$$F_z \approx 0 \tag{1}$$

$$F_x = \frac{M_{z1}}{l_2} + \frac{M_{z2}}{l_3} + \frac{1}{l_1}\left(M_{y1} + M_{y2}\right) \tag{2}$$

$$F_y = \frac{1}{l_1}\left(M_{x1} + M_{x2}\right) \tag{3}$$

F_y is puncture reaction force. F_x is direction of needle de-

Fig. 7. CT Image of Deflected Needle

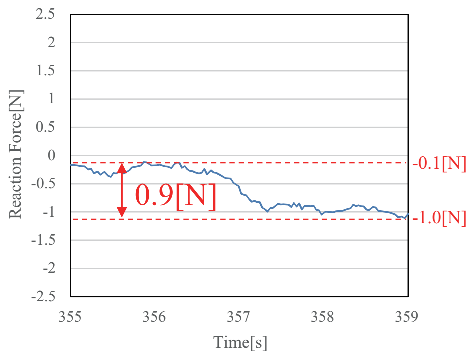

Fig. 8. F_x in the Case of Deflecting Needle

flection. When needle deflects, we can calculate theoretical value of F_x from displacement based on equations (4,5).

$$I = \frac{\pi d^4}{64}, \tag{4}$$

$$F_x^* = \frac{3EI\delta}{l_E^3}. \tag{5}$$

Here, F_x^* is the theoretical value of F_x, l_E is the whole length of needle, E is the Young's modulus, I is second moment of area, d is diameter of needle includes needle guide and δ is displacement of deflected needle tip. Parameters which are required in these equations (1) to (5) are shown in TABLE 1.

Here, CT image of deflected needle in animal experiments is shown in Fig. 7. Displacement of deflected needle tip is 8.0[mm], which is measured on CT image (in the CT image, one pixel is approximately 0.4[mm].). Therefore the value

Table 1. PARAMETERS FOR CALCULATION OF FORCE VALUES

Parameter	Value
l_1	0.1175[m]
l_2	0.08105[m]
l_3	0.14005[m]
l_E	0.0075[m]
d	0.0011[m]
E	200

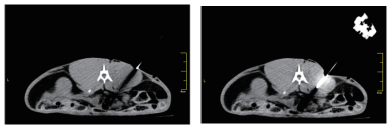

(a)

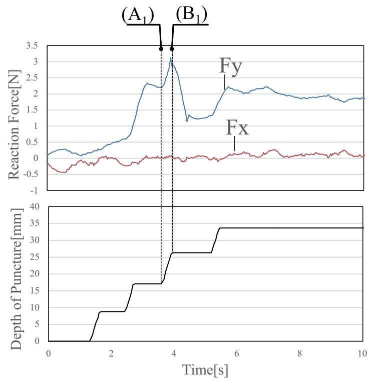

(b)

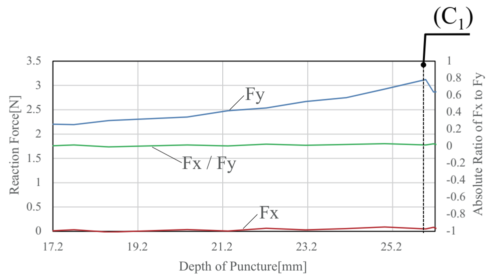

(c)

Fig. 9. Experimental data of puncture far from bone. (a) is CT image, (b) is reaction force and depth of puncture, and (c) is relationship between reaction force and depth of puncture. In (c), the horizontal axis shows depth of puncture, the vertical axis of the left side shows the value of reaction force, and the right side one shows the absolute ratio of F_x to F_y.

of F_x^* is calculated as 0.8[N]. The graph of F_x measured by force sensors of this case is shown in Fig. 8. The value of F_x is approximately 0.9 [N] when the needle deflects in the graph. Comparing F_x value and F_x^* value, we can calculate feasible F_x value by equation (2,5).

3.2 Results

Rabbit's body is tender than human's, so needle cannot be inserted into rabbit via surface skin even if the doctor tries to insert needle by his hand. Therefore needle inserting point which is marked at planning stage was incised epidermally. Experimental results are shown in Fig. 9 to Fig. 11.

Experimental results in the case of succesful puncturing is shown in Fig. 9. At CT image shown in Fig. 9(a), it is confirmed that needle tip position has reached to target point. Reaction force is shown in Fig. 9(b). It is confirmed that needle is inserted deeper, F_y icreases rapidly. On the other hand,

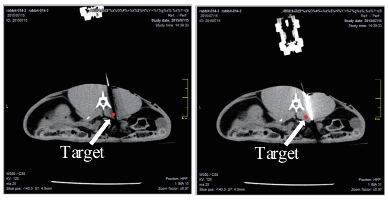

(a)

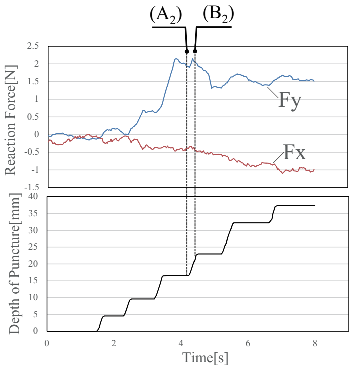

(b)

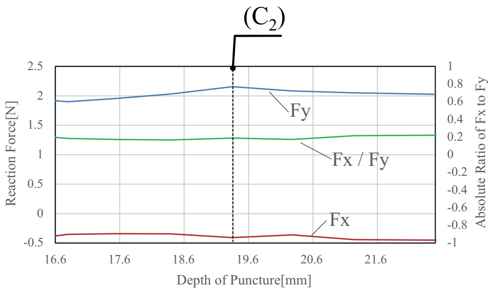

(c)

Fig. 10. Experimental data of puncture close to bone. (a) is CT image, (b) is reaction force and depth of puncture, and (c) is relationship between reaction force and depth of puncture. In (c), the horizontal axis shows depth of puncture, the vertical axis of the left side shows the value of reaction force, and the right side one shows the absolute ratio of F_x to F_y.

the value of F_x is almost constant. In this case, considering from these facts, reaction force was applied to only direction of puncture axis. Fig. 9(c) is the graph of showing the relation between depth of puncture and reaction force from A_1 to B_1. As the needle goes forward to forward, F_y value increases linearly. Therefore surface skin of rabbit's body tissue has spring property. But after depth of puncture reaches to C_1, the spring property is broken because surface skin succumbs to puncture force. We can conjecture that destruction of spring property is caused by needle penetration.

Fig. 10 shows experimental result, under the condition path plan of needle goes through issue close to bone. In this case, trajectory of needle insertion was affected by deflection of needle. This fact is confirmed from Fig. 10(a). In

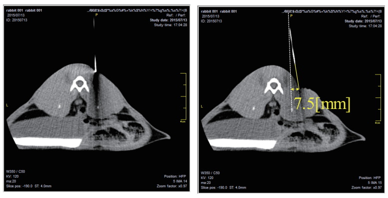

(a)

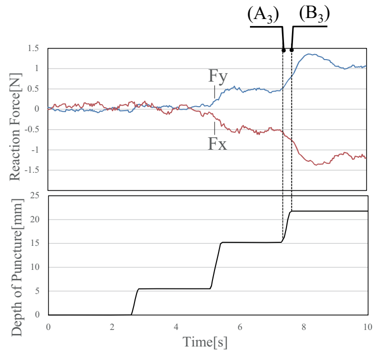

(b)

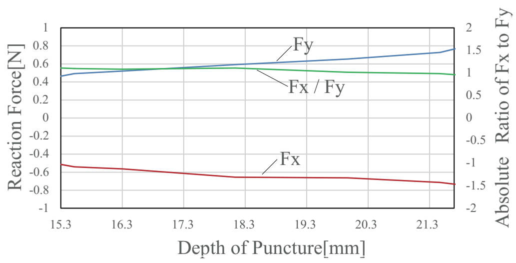

(c)

Fig. 11. Experimental data of failed puncture. (a) is CT image, (b) is reaction force and depth of puncture, and (c) is relationship between reaction force and depth of puncture. In (c), the horizontal axis shows depth of puncture, the vertical axis of the left side shows the value of reaction force, and the right side one shows the absolute ratio of F_x to F_y.

Fig. 10(b) the transition of the F_x finally reaches about 1[N]. We can conjecture that the increase of F_x is caused by needle deflection. Fig. 10(c) shows the force between A_2 and B_2 in a same way of Fig. 9(c). The spring property is shown until depth of puncture reaches C_2, and after that, the spring property is broken. Comparing Fig. 9(c) and Fig. 10(c), absolute ratio of F_x to F_y in the latter graph is larger than that in former.

Failed puncture data which tried insertion from the surface skin without incision is shown in Fig. 11. Deflection of surface skin and needle is confirmed from Fig. 11(a). In the graph of reaction force shown in Fig. 11(b), transition of F_x and F_y show the same shape. And in Fig. 11(c), destruction of spring property is not shown and absolute ratio of F_x to F_y is almost 1.

We assume the model of rabbit's tissue as shown in

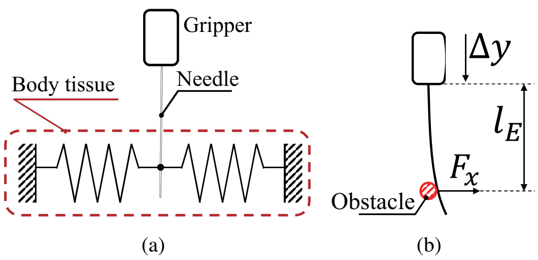

Fig. 12. (a) Model of rabbit's body tissue and (b) model of failed puncture.

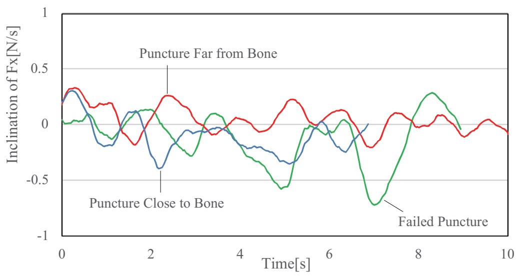

Fig. 13. Inclination of F_x

Fig. 12(a). If needle penetrates rabbit's skin, needle is constrained by spring property of rabbit's body tissue. When deflection force applies to needle, spring property prevents the force increasing because needle tip displaces. Therefore inclination of F_x cannot increase rapidly. Next, we derived the failed puncture model as shown in Fig. 12(b). In this figure, Δy means the velocity of puncture. When puncture failed, needle deflection is performed as a certain obstacle prevents the trajectory of needle. Therefore needle is punctured deeper, deflection force applies to more near point of needle's root. In this case, considering with equation (5), δ is constant and l_E decreases linearly if Δy is constant. So F_x varies on the order of x^{-3}. Then we conjecture that F_x varies more rapidly in the case of failed than in the case of penetrating. Finally, we focused the inclination of F_x for time which is shown in Fig. 13. Inclination value of failed puncture is only under -0.5. In these cases, if we set threshold value to -0.5, it can be predicted whether deflection of needle will increase or not.

4 CONCLUSION

In this paper, overview of Robotic IVR and animal puncture experiment is described. IVR robot which has developed has succeeded to insert needle to rabbit's body tissue. When needle is inserted to rabbit, deflection of needle caused by softness of rabbit's body tissue occured. And trajectory of needle will be affected by this problem. We can conjecture that this problem will occur also at the time of inserting needle to human. When a needle penetrates surface skin, destruction of spring property of skin was confirmed. In order to detect deflection of needle, force on lattel direction is significant. If inclination of force on lattel direction becomes over threshold, the system can detect the deflection of inserting needle.

ACKNOWLEDGMENTS

This work was supported by Research on Development of New Medical Devices 15652923 from AMED.

REFERENCES

[1] Japan IVR Society, "http://www.jsivr.jp/"

[2] Takao Hiraki, Tetsushi Kamegawa, Takayuki Matsuno, Susumu Kanazawa, "Development of a Robot for CT Fluoroscopy-guided Intervention : Free Physicians from Radiation", Jpn Journal of Intervent Radiol, 20:375-381, 2014.

[3] Takao Hiraki, Hideo Gobara, Hidefumi Mimura, Shinichi Toyooka, Hiroyasu Fujiwara, Kotaro Yasui, Yoshifumi Sano, Toshihiro Iguchi, Jun Sakurai, Nobuhisa Tajiri, Takashi Mukai, Yusuke Matsui, Susumu Kanazawa, "Radiofrequency Ablation of Lung Cancer at Okayama University Hospital: A Review of 10 Years of Experience", Acta Med., Vol.65, No.5, pp. 287-297, Okayama, 2011.

[4] Dan Staianovici, Kevin Cleary, Alexandru Patriciu, Dumitru Mazilu, Alexandru Stanimir, Nicolae Craciunoiu, Vance Watson, Louis Kavoussi, "AcuBot: A Robot for Radiological Interventions", IEEE TRANSACTIONS ON ROBOTICS AND AUTOMATION, VOL.19, NO.5, pp.927-930, OCTOBER 2003.

[5] Benjamin Maurin, Bernard Bayle, Olivier Piccin, Jacques Gangloff, Michel de Mathelin, Christophe Doignon, Philippe Zanne, Afshin Gangi, "A Patient-Mounted Robotic Platform for CT-Scan Guided Procedures", IEEE TRANSACTIONS ON BIOMEDICAL ENGINEERING, VOL.55, NO.10, OCTOBER, 2008.

[6] Joachim Kettenbach, Gernot Kronreif, Michael Figl, Martin Fürst, Wolfgang Birkfellner, Rudolf Hanel, Wolfgang Ptacek, Helmar Bergmann, "Robot-Assisted Biopsy Using Computed Tomography-Guidance Initial Results From In Vitro Tensts", Investigative Radiology, Volume 40, Number 4, pp.219-228, April 2005.

[7] Hirotaka Nakaya, Takayuki Matsuno, Tetsushi Kamegawa, Takao Hiraki, Takuya Inoue, Mamoru Minami, Akira Yanou, Akio Gofuku, "Development and Evaluation of Phantom for CT-IVR", JSME Conference on Robotics and Mechatronics, Toyama, Japan, 2014.